Double-Pulsed Gradient Spin-Echo from DTI in the Fibromuscular Stroma of the Prostate

Scott A. Willis[1], Timothy Stait-Gardner[1], William S. Price[1], and Roger Bourne[2]

[1]*Nanoscale Organisation and Dynamics Group, School of Science and Health, University of Western Sydney, Sydney, NSW, Australia,* [2]*Discipline of Medical Radiation Sciences, Faculty of Health Sciences, University of Sydney, Sydney, NSW, Australia*

TARGET AUDIENCE – Researchers studying diffusion in biological tissues with tensors and double-pulsed gradient spin-echo methods.

PURPOSE – Self-diffusion, the most elementary form of molecular transport in solutions, reports on binding events, restrictions (e.g., porous rock, biological cells) and anisotropies of the system, and can be measured using pulsed gradient spin-echo (PGSE) NMR (e.g. [1]). Double-pulsed gradient spin-echo (DPGSE) was first proposed to probe pore eccentricity by Cory *et al.*[2]. DPGSE is useful for probing molecular dynamics and pore sizes in biological tissues, giving more information than single PGSE measurements.[3-5] The purpose of this work was to investigate the angular DPGSE profiles (i.e., using equivalent gradient strengths for each encoding-decoding block of the DPGSE but with varying angular separation, i.e., gradient vectors $\mathbf{g}_1$ and $\mathbf{g}_2$ or 'q' vectors $\mathbf{q}_1$ and $\mathbf{q}_2$ with the same magnitude but with $\mathbf{g}_2$ or $\mathbf{q}_2$ at an angle ψ to a fixed $\mathbf{g}_1$ or $\mathbf{q}_1$) in prostate tissue and use DTI results to simulate the expected DPGSE profile for a 'one-voxel' DPGSE measurement (i.e., treating the sample as one imaging voxel).

MATERIALS AND METHODS – Two formalin fixed prostate samples (~4 mm diameter) from two regions of a prostate were used. A core ~8 mm in length was taken from the central zone (CZ) and was all fibromuscular stroma (FMS). A core ~7 mm in length was taken from the peripheral zone (PZ) and was found to be normal glandular tissue (NGT). The cores were saturated with a buffer solution, containing 0.5% NaCl with a small amount of formalin and 0.2 %v/v Magnevist®, and then transferred into Fomblin® and 5-mm coaxial NMR tubes. The Fomblin® was observed to penetrate into the largest pores/glands of the PZ sample while the FMS of both samples only contained buffer.

DPGSE and DTI measurements were performed at 20 °C using a Bruker Avance 500 MHz NMR spectrometer with a Micro5 probe and 5-mm insert. DPGSE experiments for the entire sample were typically performed for 25 angles (0 to 360°) and 6 direction combinations (**Fig. 1**) to obtain 'one-voxel' DPGSE 'fingerprints' for the anisotropies present. Typically the mixing time was 4.6 ms, the gradient durations and diffusion times were $\delta_1 = \delta_2 = 4$ ms and $\Delta_1 = \Delta_2 = 30$ or 50 ms, and $q_1 = q_2 = 26001$ m^{-1} (where $q_{1,2} = \gamma\delta_{1,2}g_{1,2}/2\pi$). Several DPGSE and DTI (PGSE) measurements were made for different physical orientations (i.e., physical rotations about the axis of the sample tube) for the CZ core sample and one set of DPGSE and DTI results were obtained for the PZ sample. 'Whole sample' DTIs (i.e., one 9 – 9.5 mm slice) with in-plane resolution of 150 × 150 μm^2 were measured for both samples. 3D DTIs with voxel size of 180 × 180 × 360 μm^3 were measured for the CZ sample in Fomblin® and the PZ transferred back into buffer (i.e., surrounded by buffer with large pores/glands filled with buffer). Typical parameters for the DTI were: TE 14.1 or 14.6 ms, TR 1.5 s, 8 directions similar to Jones *et. al.*[6] (see also [7]) but including the extra direction of [-0.577, -0.577, 0.577], 1 A0 image, 16 *b*-values (250 – 1300 s mm^{-2}) for 'whole sample' and 3 *b*-values (50, 150, 250 s mm^{-2}) for 3D, $\delta = 1$ or 1.5 ms, $\Delta = 10$ ms and 1 scan ('whole sample') or 6 scans (3D) per image/slice.

'One-voxel' DPGSE profiles were predicted using DTI results (i.e., those measured with the sample in Fomblin®). The angle rotated from the reference DTI position was included before prediction of the DPGSE if it was measured with the sample in a different physical orientation to that of the DTI. DPGSE profiles were predicted using equations based on a diffusion tensor/anisotropic diffusion approach similar to [4, 8] but in exponential form and distinct from other approaches.[9, 10] This approach used three rotation angles and three principal diffusivities for each voxel (or orientation region if sorted and averaged). 'One-voxel' DPGSE profiles were predicted using a summation of the DPGSE profiles predicted for every voxel in the DTI measurements (but could also have been done by a summation of the average orientations and proportions in the sample).

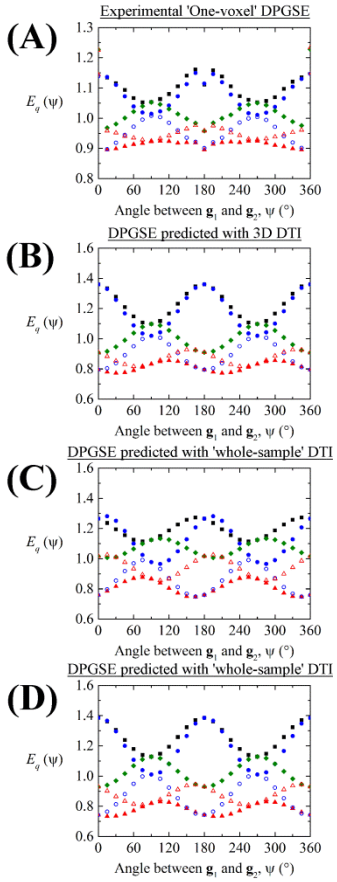

Figure 1 Example results obtained from 'one-voxel' DPGSE measurements and predictions from DTI for the CZ-FMS core sample. **(A)** Experimental DPGSE. DPGSE predicted from **(B)** 3D and **(C)** & **(D)** 'whole sample' DTI results. $\mathbf{q}_1/\mathbf{q}_2$: *x*/*x*-*z* (■), *x*/*x*-*y* (●), *y*/*y*-*z* (▲), *z*/*x*-*z* (◆), *y*/*x*-*y* (○) and *z*/*y*-*z* (△).

RESULTS AND DISCUSSION – The CZ-FMS and PZ-NGT prostate core samples had different fibre orientations (i.e., of the largest eigenvectors) throughout the samples as could be expected. The CZ-FMS sample was observed to contain two main orientation regions compared to the PZ-NGT sample which had several orientations that weaved around the gland acini. 'One-voxel' DPGSE results for the fibrous parts of both samples showed patterns expected from the diffusion tensor/anisotropic diffusion approach. The results from the DTI measurements could be used with the base exponential form of the signal intensity to simulate the expected result from a 'one-voxel' DPGSE measurement (**Fig. 1**). The data for the 'one-voxel' DPGSE and the DTI-predicted 'one-voxel' DPGSE were each normalised to their means (i.e., mean of all six profiles for each dataset) which kept both the information of the phase of the profiles and relative positions of the profiles for the different $\mathbf{q}_1/\mathbf{q}_2$ measured. There were some differences in terms of slight phase shifts, span of the profiles and the position of the un-normalised profiles. These could be due to the DTI tensors being inherently more noisy (i.e., imaging) and the accuracy of the tensor elements and the eigenvector orientations would influence the results (i.e., the DPGSE equations are sensitive to the tensor elements and orientations for both span and phase of the profiles). Another difference might be due to any time dependency of the diffusion (i.e., DTI were measured with a shorter diffusion time). Additionally, the predictions were made with no additional weighting or offsets and only the base exponential form with summation over all DTI voxels was used. Fluctuations in the fibre/tensor orientations will be included as future works. Interestingly, the results using the 3D DTI and the 'whole sample' DTIs for the CZ-FMS showed similar predictions for the DPGSE (again, slight differences are likely due to the estimation of the orientation with respect to each experiment).

CONCLUSIONS – These results show that the FMS in the prostate gives rise to clear 'one-voxel' DPGSE profiles that can, for the most part, be simulated using diffusion tensor results from DTI measurements. It was seen from the prediction of the DPGSE profile from the DTI results for both samples, that the models need to be extended or modified to include other factors (e.g., offset, additional weightings for noise in the tensor results, fluctuations in the orientations), although using only the base exponential form for the signal intensity reasonably models the features in the 'one-voxel' DPGSE 'fingerprints'. This study highlights the ability of the DPGSE to include all information about the orientations present in 'one-voxel' and the utility of the diffusion tensor/anisotropic diffusion approach to predict the experimental DPGSE for a real tissue sample.

REFERENCES – [1] Price, W. S., *NMR Studies of Translational Motion*. Cambridge University Press: New York, 2009. [2] Cory, D. G., *et al*., *Polym. Prepr. (Am. Chem. Soc., Div. Polym. Chem.)* **1990,** *31*, 149-150. [3] Shemesh, N., *et al*., *NMR Biomed.* **2010,** *23*, 757-780. [4] Finsterbusch, J., Chapter 6 - Multiple-Wave-Vector Diffusion-Weighted NMR. In *Annu. Rep. NMR Spectrosc.*, Webb, G. A., Ed. Academic Press: 2011; Vol. 72, pp 225-299. [5] Callaghan, P. T., Double Wavevector Encoding. In *Translational Dynamics and Magnetic Resonance: Principles of Pulsed Gradient Spin Echo NMR*, Oxford University Press: Oxford, 2011. [6] Jones, D. K., *et al*., *Stroke* **1999,** *30*, 393-397. [7] Skare, S., *et al*., *J. Magn. Reson.* **2000,** *147*, 340-352. [8] Finsterbusch, J.; Koch, M. A. *J. Magn. Reson.* **2008,** *195*, 23-32. [9] Özarslan, E.; Basser, P. J. *J. Chem. Phys.* **2008,** *128*, 154511. [10] Özarslan, E. *J. Magn. Reson.* **2009,** *199*, 56-67.

Grant Support: This project is supported by an NHMRC Project Grant (1026467).